

The Higgs Decays and Cusps

Gudrun Kalmbach H.E.*

*MINT, PF 1533, D-86818 Bad Woerishofen, Germany

Received March 26, 2021; Revised April 25, 2021; Accepted April 27, 2021

ABSTRACT

In a new evolution after a big bang, coordinate generation and annihilation are discussed, using cross products, projections and fiber bundle maps. As new force color charges, independent of QCD, with rgb-gravitons are related to the octonion G-compass. New measuring Gleason operators as GF are described. Decay geometries for systems are set on dihedrals with n th roots of unity as characteristic polynomials.

DARK MATTER, OCTONIONS AND GF

Dark matter Q is presented in the MINT-Wigris model as a Horn torus with energies inside. If energy is stored as 1-dimensional retracted quark lemniscates P_j , arranged in retracted nucleons as butterflies P with six wings their radius r 'inversion as decay of the Horn torus is at the Schwarzschild radius R_s of Q where they get in the universe a radius r with $r = R_s$. The change of dimension from 1 to 3 space dimensions xyz is due to adding an eigen rotation of the system, called spin. This is by projective duality, using a correlation in a real projective space P^5 . To a point O as origin of space xyz-coordinates corresponds a 4-dimensional hyperplane as spacetime with xyzt-coordinates. The xy-plane is taken as the aggression disk of Q with origin O. The above radius inversion is at a (radius normed) unit circle U (1) of an octonion 7th Kaluza-Klein rolled coordinate. To a point as barycenter of the universes nucleon P (or P_j) corresponds a common center P 'of the lemniscates with the above radius inversion. Higgs bosons or field can set a mass scalar as kg-weight at P, P 'which is an octonion 5th coordinate. If octonion coordinates are listed in tuples of indices, there are at this decay steps 123457 for six octonion coordinates.

Inversion of time 4 to 6 as frequency $f = 1/\Delta t$ is for speeds $v = \Delta x/\Delta t$. Dark matter in Q has speed $v > c$, inverted to universes matter speed to $v < c$ in $v = c$.

Octonions have in 1234567 seven Pauli matrix extended base triples (lines in **Figure 1** with three points as GF triple), Gleason operator frames GF as measuring apparatus, listed in the Fano memo (**Figure 1**). The spin triple 123 matrices belong also to the weak interactions WI as SU (2) generators. Triples like 123 are measuring operator frames. They have weights attached at their three vectors, for spin as

123 it is length/meter in space. For gravity a SU (3) strong interaction SI triple 126 GF, using GellMann extended Pauli matrices $\lambda_{1,2,3}$, is added which makes a space with 7 octonion variables and 3 parameters for three color charges red 1r, green 2g and blue 6b. The octonion coordinate e_0 1r (an eigenvector of a matrix G, also for wave length λ or radius r), noted as 0 if no confusion numerical occurs, is obtained by bifurcating 3 into a plane 03. This correlation of a line 3 with a plane 03 is in a 4-dimensional P^4 space. The relation with P^5 is that to P^4 is added a real 5-cell R^5 . It is for a Higgs field, used in [10] for a Kaluza-Klein projective unification POT (as force and potential) of the electrical EM with the gravity GR potentials EM (pot), E(pot). They are a driving motor for quarks, having a 2-roll mill inner plasma flow about their two foci of the central lemniscate (**Figure 2**). P^5 has as projections 1234 for EM (pot), EM and the weak interaction WI. There are two more projections of P^5 . 1256 is for E(pot), GR which makes the real 6-, complex 3-dimensional octonion subspace 123456. The third projection is 3456 for CP^2 as complex 2-dimensional space for nucleons and atomic kernels. It arises as base of a fiber bundle $g: S^5 \rightarrow CP^2$ with fiber S1 (U (1) 7). 1234 has the Hopf fiber bundle with fiber U (1) h: $S^3 \rightarrow S^2$. These unit spheres S_n in a real space of one dimension higher are topological 1-point ∞ compactifications of a real space R_n

Corresponding author: Gudrun Kalmbach H.E., MINT, PF 1533, D-86818 Bad Woerishofen, Germany, E-mail: mint-01@maxi-dsl.de

Citation: Gudrun Kalmbach H.E. (2021) The Higgs Decays and Cusps. J Chem Sci Eng, 4(1): 189-196.

Copyright: ©2021 Gudrun Kalmbach H.E. This is an open-access article distributed under the terms of the Creative Commons Attribution License, which permits unrestricted use, distribution, and reproduction in any medium, provided the original author and source are credited.

with a stereographic map $st_n: S^n \rightarrow R^n$ from ∞ as central projection.

For the rgb-graviton are added to octonions with 1r as orthogonal base vectors the 2g, 6b parameters, generating to R^5 as cell of P^5 a 5-dimensional complex extended space C^5 . In projective notation, real (or complex) to $P^1 \equiv S^1$ ($C^1 \equiv S^2$, the unit sphere in R^2) are topological added n-cells, $n = 2,3,4,5$, in form of $X^k = Y^k U X^{(k-1)}$, $X = P$, $Y = R$ ($X = CP$, $Y = C$). Octonions and $SU(3)$ correspond to $C4$ and $C4$ is extended, by using the complex cross product, to $z_5 = (2g,6b) = z_1 xz_2 xz_3 xz_4$. The dark matter Q aggregation disk as octonion 12 xy-plane is after a Higgs decay of Q extended to a complex 2-dimensional space with coordinates 12(2g) (6b). The coordinate 2g is for a phase angle φ_0 and exponential function $\exp(i\varphi_0)$, adding to waves $\exp(i\omega t)$ with t time and angular frequency $\omega = 2\pi f = d\varphi/dt$ (f frequency) a phase translation $\exp(i(\omega t + \varphi_0))$. The angle as θ on 3 for the angular position of a compass needle 0 occurs also between two rays as in **Figure 2** for GR generated orthogonal and spiralic projections. If the rays are in direction of an octonion coordinate $g_{a,b}$ which belongs to two different systems a,b, the measures of their eigenvectors on g_j are rescaled by $\cos \varphi_0$ (contracted or extended) when observed on g_k , $k \neq j$ (**Figure 3**). The third rgb-graviton parameter of z_5 6b is for measuring frequency through winding numbers $\omega = 2\pi f = d\varphi/dt$ with $f = 1/\Delta t = n$, $n = 1, 2, \dots$ natural numbers. The counting comes from the linear universal cover R^7 of S^1 as Kaluza-Klein rolled $U(1)$ symmetry of the electromagnetic interaction EMI. In 2π circulations about S^1 , counted by n through a residual complex S^1 contour integration, the EMI frequency has for $\exp(i\omega t)$ the period $2\pi n$ which rolls R up to S^1 ; the circulation time is $\Delta t = 1/n$. time inversion to f quantizes time, for instance as a Calderon or the Planck time. As triple (ω, t, f) 346 is a spin-like Gleason operator GF frame as an orthogonal base triple. For 345 can be used 3 in Joule as

rotational energy $E(\text{rot})$, 4 as time measured in seconds s or magnetic field strength $E(\text{magn})$ measured in Wb, for 6 measured as inverse time in s-1. For 0 as 1r 037 as $(r, \theta, \exp(i\varphi))$ can serve as a compass 07 extended measuring GF. For 2g a measuring GF triple is 2(2g)7 as $(\varphi, \theta, \exp(i\varphi))$ 237. θ is a turning spherical angle towards the space z-axis 3. As trifurcations appear 2,3. 2 for heat has the Fano 246 GF, 3 for rotation the Fano 347 GF, but the trifurcations are for 2 as $[2, \varphi_0, 7]$ and for 3 $[\omega, t, f]$. The GF 's can be extended for quasiparticle presentations.

As new force on 0 is suggested the color charge force cc with rgb and conjugates $c(r)c(g)c(b)$ as six G-compass values (**Figure 4**); the GF triple is 126, the rgb-gravitons; 2 as 2g and 6 as 6b are z_5 parameters, not variables. Among the catastrophes, the cusp fits to 126 as (1r) (2g) (6b) with 1r as variable.

The aggregation disks xy-plane E_{xy} is also extended by the octonion 7 coordinate. It was used as linear universal cover of the unit circle $U(1)$ in E_{xy} . Wave length (meter for space) is quantized by spin vector lengths, using the Planck constant h. R is presented as helix line on a cylinder with $U(1)$ as transversal section. There are energies and measuring GF 's associated with all octonion coordinates EM (pot) Ampere 1 with 123 GF (also for meter); Kelvin k for 2 E(heat) with GF 246, E(rot) Joule 3 with 346 or 347 GF; E(magn) with GF 145 or time 4 with Wb or s; E(pot) kg 5 with 257 GF; E(kin) as frequency 6 with s-1 and GF 356, and 7 cd EMI with GF 167. An additional strong interactions GF was 126 for GR rgb-gravitons as superposition of three cc whirls for the nucleons neutral color charge. Quarks in nucleons have always r,g,b color charges in gluon exchanges which change the states and locations in nucleons. Counting also 037, 237, 346, there are 11 GF in use, more can be invented for quasiparticles (32 in a list).

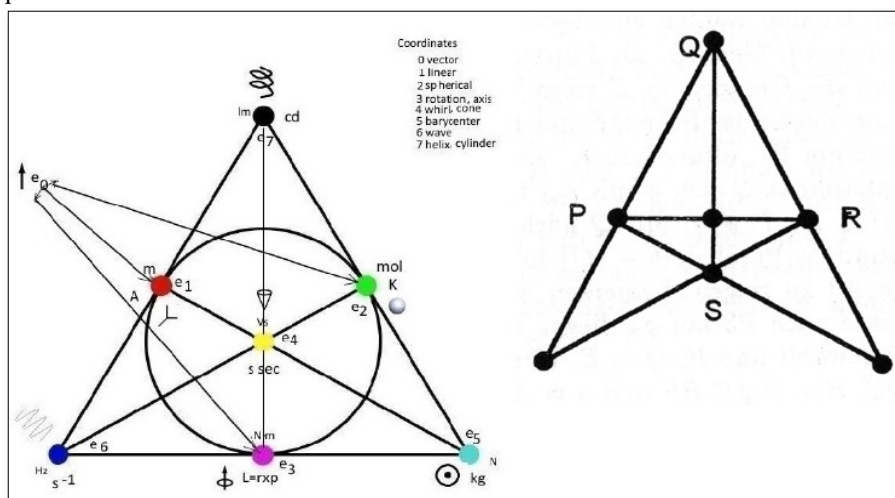


Figure 1. Fano memo [1], discrete affine plane with 4 points P, Q, R, S and 4 lines, extended to the projective plan with 7 points and 6 lines, the circle through e1,2,3 at left as 7th line is not drawn.

Flows are shown in **Figure 2**.

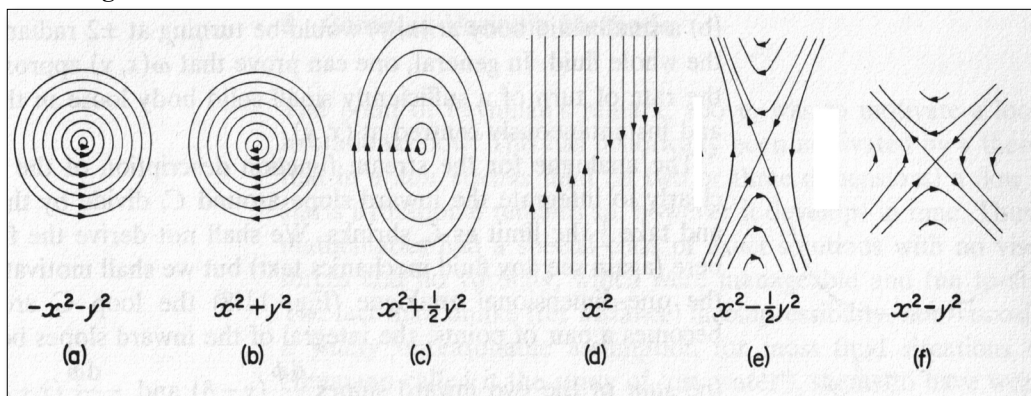


Figure 2. Flows (from [3]), (equi-) potential or field lines, (e) 2 roll mills for quarks, (f) roll mill for the WI rotor.

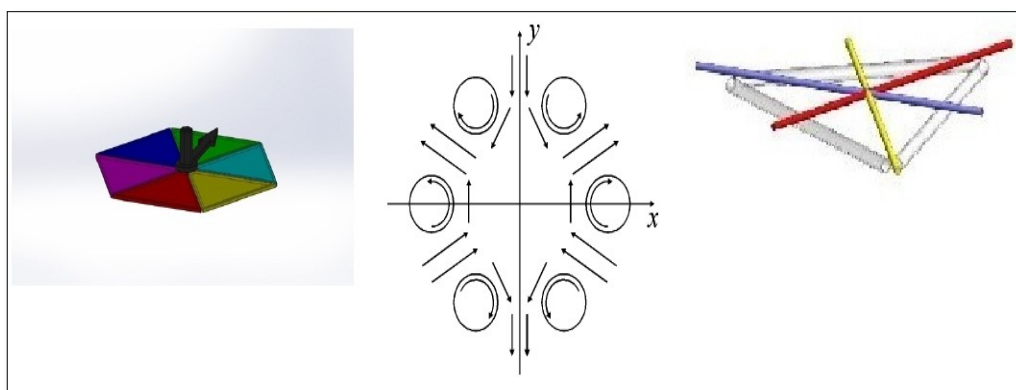


Figure 3. G-compass, 6 roll mills [5,6], barycentric coordinates.

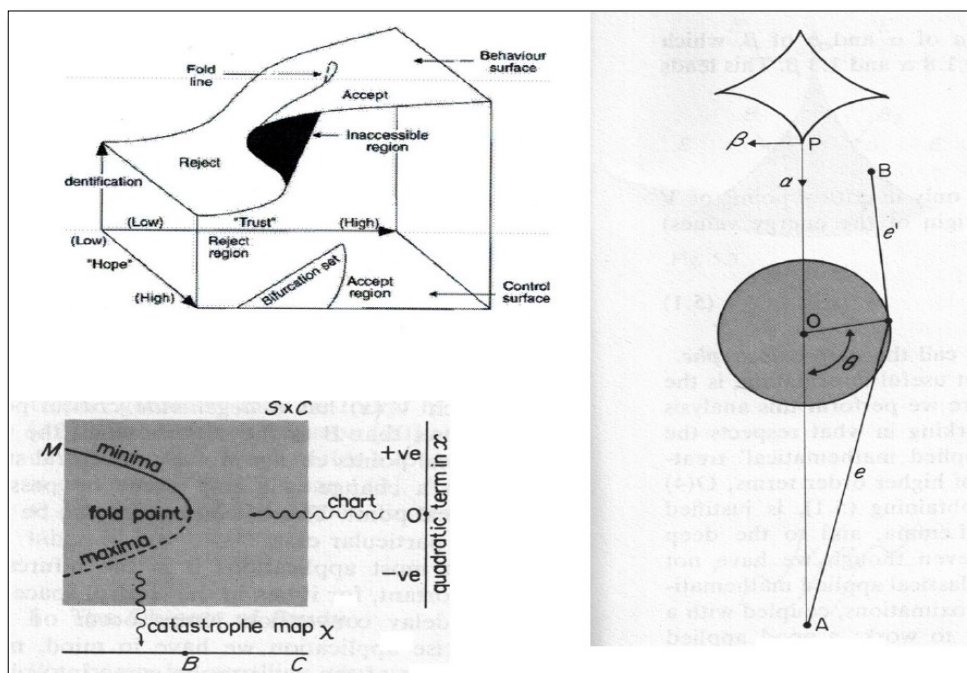


Figure 4. Cusp, fold, Zeeman gravitational machine.

In the first line of the **Figure 5** are the spherical SI coordinates, possibly 7- (or 8-)dimensional extended with exponential/polar coordinates. In the second line are the linear Pauli/Euclidean coordinates, in the third line a distribution of color charges to the SI coordinates. The fourth (fifth) line contains the D_3 (SU (2) Pauli) MTs as cross ratios. Their matrix names are in the sixth line, together with the Einstein matrices. The following line is a numbering for a strong 6-fold integration series (also the Fano figures numbers which are for octonions). The next line contains the Planck numbers. Energy vectors are in the third to last line and the next line contains natural constants and three more operators, C (conjugation for quantum numbers), T (time reversal) and P (space parity) of physics. The **Figure 5** is from the 1998 book of the author, revised by adding at left and right two columns for the octonion extension 01234567 of the old color charge space 123456, extending spacetime 1234. The first row is introduced for color charges as own energy force $E(cc)$, having as values the complex six cross ratios in line 4 for color charges in line 3. A G-compass for 2x2-matrix extension for octonion coordinates is added at left with an eigenvector e_0 . All coefficient matrices of complex cross ratios in the 4th line get an eigenvector attached for setting their energy units, listed in 8th line. In the third line of the first column is in the third row listed a turning angle for the G-compass needle ea . It uses the k th roots of unity on $\exp(i\theta)$ as the G-compass boundary, a unit circle, for discrete turns. To this belong weak decays of the SU (2) geometry S^3 , its Heegaard decompositions into two solid handle bodies of genus k . Manifolds are bounding them in form of k tori glued at a 2-dimensional sphere S^2 . Drawn on U (1) as k points for a dihedral D_k , the symmetries of order $2k$ describe dynamical rotors for the basic interactions. As points, $k = 1$ presents a monopole where an energies charge can be set, $k = 2$ is for dipoles, magnetic momentum for instance, $k = 3$ is for the quark triangle of a nucleon, $k = 4$ (powers of the imaginary

number i) is a weak WI rotor and $k = 6$ is a strong SI rotor. The WI rotor is driven by the weak interaction WI and a unified POT force of the electrical and gravity potentials. To this is added the strong interaction force SI for the SI rotor. This one describes dynamically a quark-gluon plasma inside a nucleon. It is constructed as 6 roll mills in catastrophe theory and has as potential the elliptic umbilic with 2 variables and 3 parameters. The parameter interpretation of the octonion coordinates is used in the table: φ 2 has two parameters as φ_0 in the first row and in $\exp(i\varphi)$ in the last row. The parameters of θ are in the first row and in the last row as angular frequency (speed) = $2\pi f = d\varphi/dt$, listed as f . Time t has T in the last row as parameter. In the first row is listed a 2x2-matrix G which is the order 6 scaled coefficient matrix of $E(rot)$. It is interpreted as an acoustic or gravitational, spiralic rgb whirl rotation circulation time of a rgb-graviton as superposition of three-color charge whirls r red, g green, b blue, observed as neutral color charge of nucleons. The triples count for 3-dimensional orthogonal base measuring frames GF like spin which measures length in space as meter. In the 8th line are listed the names for energies and their GF triples (last line) are found in the authors 2019 book and in her older publications. An octonion Fano memo exists seven GF, rgb as 126 is added to them.

In the last column, f counts natural numbers n (and 0) for winding numbers about a circle $\exp(i\varphi)$ (in the 5th line). Below is R for the real number plane as universal cover of the U (1) circle (6th line). R winds above U (1) as helix line on a cylinder and $2\pi m$ counts its winding numbers as period of $\exp(i\varphi)$. T in the fourth line is the circulation time for n windings. The linear octonian coordinate is 7 (7th line). The measuring force unit is candela cd . The coordinate 7 presents the electromagnetic interaction EMI energy.

e_0	r	φ	θ	ict	iu (f)	iw (m)	$f = n$
	$x \in \mathbb{R}$	$iy \in i\mathbb{R}$	$z \in \mathbb{R}$				
θ	r	g	\bar{g}	\bar{b}	b	\bar{r}	R
G	z	$\frac{z}{-z-1}$	$\frac{-z-1}{z}$	$(-z-1)$	$\frac{1}{-z-1}$	$\frac{1}{z}$	$T = 1/n$
φ_0	$\frac{1}{z}$	$-\frac{1}{z}$	$-z$	z			$e^{i\varphi}$
	$id; \sigma_1$	$\alpha\sigma_1; \sigma_2$	$\alpha^2; \sigma_3$	$\alpha^2\sigma_1; id$	$\alpha; \delta$	$\sigma_1; id; \beta$	U(1)
0	1	2	3	4	6	5	7
rgb	length λ_P	temp. T_P	dens. ρ_P	time t_P	ener. E_P	mass m_P	cd
E(cc)	EM_{pot}	E_{heat}	E_{rot}	E_{magn}	E_{kin}	E_{pot}	EMI
γ_G	e_0, ϵ_0	k, C	N_A	μ_0, T	h	$R_{S,P}$	c
126	123 spin	246	347	145	356	257	167

Figure 5. Cusp, fold, Zeeman gravitational machine.

Higgs decay, orbits and cusps

For the weak interaction, the Heegaard decompositions of S^3 into solid brezels of genus $n = 0, 1, 2$, are for decomposing S^3 into two handle bodies of genus n where $n = 0$ gives two solid balls, with boundary S^2 , splitting S^3 at an equator.

The big bang or dark matter Higgs boson decay is different. The xy -plane of it gets extended by the real cross product to the GF 127. The unit circle for 7 (set $[x, y, 0]$ in 12) is extended to a cylinder in 127 with axis 7. The exponential function $\exp(i\omega t)$ oscillation is for EMI waves extended to $\exp(i(\omega t + xk + \varphi_0))$, φ_0 a phase angle as parameter, $k = 2\pi/\lambda$ wave number, λ wave length as parameter and x substituting for 7 as expansion of the wave on its world line with speed $c = v = \Delta x/\Delta t$. A projective space extension is $[x, y, 9, \varphi_0, 10, \lambda]$. In the SI GellMann λ_j matrices λ_8 is replaced by λ_9, λ_{10} and their extended GF triples 459, 67(10). If complex extensions of spacetime coordinates $z_1 = (z, ict)$, $z_2 = (x, iy)$ with the complex cross product to 56 $z_3 = (m, f) = z_1 \times z_2$ is substituted, there are three SI 4-dimensional projection spaces 1234 for WI/EM, 1256 for GR and 3456 for nucleons and atomic kernels as CP^2 , as mentioned before. In complex SI 3x3-matrix extension they are $(z_1, z_2, 0)$, $(z_1, 0, z_3)$, $(0, z_2, z_3)$. Substituting the $[x, y, 9, 10]$ coordinates for a cusp catastrophe [3] potential as $V_{ab}(x) = x^4/4 + ax^2/2 + bx$ with the cusp equation $u_1^4 + t_2 u_2^2 + t_1 u_1$ and $x = u_1$, $y = u_2$ as variables $9 = t_1$, $10 = t_2$ as parameters and $x = y$ for V , the cusp geometry can be used (**Figure 4**). In the first section, the cusp parameters are interpreted as the rgb -graviton z_5 parameters $2g$ (for 9 and a spherical phase angle θ of the G-compass needles n th roots of unity positions), $6b$ (for 10 as circulation winding numbers $f = n$ frequencies ω). It means also that in the 127 EMI cylinder above the coordinate 7 is used in projection where for the complex exponential wave function only the real cosine part is observed in spacetime. This is as a finite part for the wave length a cosine oscillation like LASER with two fixed endpoints and one knode O in the middle for $\cos \pi = 0$. For the radius above inversion [4], a barycenter P is marked on the x -line of E_{xy} and mathematical inverted at a circle with radius $\sqrt{R_s}$ to P . In time P is rotating on the cylinder surface and traces out the exp wave as helix line. The start for P is marked on U (1) as φ_0 , a phase change. Its image points are connected with P and trace out the rays of the cusp with endpoints P' . In the 27 planes of 127 cosine can be interpreted as a cubic equation $4a^3 + 27b^2 = 0$ in the control space of V and the fold line $(x, -3x^2, 2x^3)$ in the catastrophe manifold M which in a plane can be substituted for $v = u^3$ replacing cosine, and having at O the uv -planes origin. There are three potential levels (figure 3), one middle unstable part $u = 0$ containing O , an upper (lower) maximum $u < 0$ (minimum $u > 0$) potential level for a GF with these 127 three potentials as threshold weights. The Zeeman matching (**Figure 4**) for GR cusp jumps of a wheel show a superposition of four hyperbolic umbilic catastrophes with potential (two

variables and three parameters) $V_{abc} = x^3 + y^3 + axy + bx + cy$.

For the Higgs decay the thresholds mean in the control space that V gets as in the weak decay of S^3 a bifurcation into two parts with an upper V_1 or lower V_2 potential level. For a mass system Q in the universe this sets the first cosmic speed $v_1^2/c^2 = |\varphi G|$, the GR potential and $v_2 = v_1 \cdot \sqrt{2}$ as second cosmic speed, using R_s of Q . Equipotential surfaces are spheres S^2 about a barycenter B and field lines for a GR flow or wave in time are rays with initial point B .

The S^2 is whirl like rotated in time as a rgb -graviton action. In reduced coordinate form of S^1 as a transversal section E of a Minowski double cone (belonging for instance to a parabolic umbilic catastrophe), for a system P orbiting about Q with speed $v = v_1$ it means that the xy -plane E with $x^2 + y^2 = 1$ as P orbit is turned in an angle β by the rgb -graviton whirl to a leaning transversal plane $E\beta$ towards the cone M such that the diagonal of an ellipse for the P orbit has a nearest point on M . It moves after one rotation on a small circle in $E\beta$ with the other endpoint of the diagonal on an opposite cone line on a large circle (**Figure 4**). The P speed-accelerating periodic φ_0 $2g$, phase changing angle is due to the Schwarzschild metric for Q . A similar angle β for the other two Einstein EMI waves changes brakes mirror like the world line of the light ray. This is due to the fact that the speed c can be not accelerated.

In changing to another direction for its world line, it can emit or absorb energy in relation to mass systems for the double lensing or redshift or when hitting matter surfaces or (potential) energy fields. For a planet rotating about a central sun Q having a common barycenter of the system inside Q it means that increasing the P speed changes β until the diagonal of the ellipse is threshold annihilated and is on the cone surface (parabola orbit of P for escape), turning β further gives hyperbola escape orbits for P . In both cases, there is no common barycenter for P, Q set by Higgs. In case of two galaxies where Higgs sets in relation to their speeds a common barycenter, rgb -gravitons make a spiralic contraction where $\cos \beta$ is used as orthogonal projection from one spiralic ray to an adjacent ray in this angle. This introduces also for a Hilbert space H presentation of 1234 the splitting of H into two orthogonal subspaces $H = U + U^\perp$ where a vector u can be written as $u = v + w$, $v \in U$, $w \in U^\perp$. Complex vectors z split into $z = x + iy = r \cdot \exp(i\varphi)$ in polar coordinates with $x = r \cdot \cos \varphi$, $y = r \cdot \sin \varphi$.

In case several mass systems such as three quarks in a nucleon uud or ddu have a common nucleon barycenter where Higgs sets a nucleon mass, there is a pendulum contraction/expansion by rgb -gravitons of the quark triangle in proportion of the three normed basic spin values $1/2; 1; 2$. This belongs to an SI rotor [1]. The quark speeds for rotation are between the cosmic speeds belonging to the nucleon barycenter B , B is the intersection of three quark-triangles, conic rotational generated barycentrically

coordinates (figure 3) and the quarks barycenter's are on a circle about B at the triangle's vertices.

If for matter waves the above wave equation constants are Schroedinger substituted for a common group speed v of the nucleon wave package, this requires that the sum of the quark mass m_0 is GF added for the nucleon mass $m = mf + m_i$, set by Higgs at B, with two other GF weights where mf comes from inner transformed frequencies (speeds) in $mf c^2 = hf$, h the Planck constant and m_i is coming from a special relativistic v rescaling of mass. The m_0 mass is about 10 percent of m .

Sudden changes, jumps, thresholds and symmetries

In the former sections, often discrete state changes occur.

The first one was radius inversion when a Higgs boson is decaying its inner dark matter to universes matter. The fold catastrophe has two potential levels for this and a potential function $V_a = x^3/3 + ax$. The catastrophe manifold has the equation $x^2 + a = 0$ for a parabola (figure 4) with a bifurcation singular point at (0,0) in a xy -plane. For two states the quadratic term V has a maximum for $x < 0$ (lower branch of the parabola) and a minimum for $x > 0$ (upper branch of the parabola). At (0,0) the threshold value for V sets the bifurcating radius inversion from upper to lower or lower to upper parabola curves. This makes a Higgs boson or black hole Q decay (or dimensional matter collapse). Involved is a correlation in P^5 .

A SI parametrized cusp space $[x, y, \phi_0, 6b]$ is extending the aggregation xy -plane R^2 of Q to a 4-dimensional real R^4 or projective 3-dimensional P^3 . For central projective projections like $st: S^2 \rightarrow R^2$ which is also used for raytracing the P_3 presentation is used. For parallels in a Euclidean space R_n , it means that they are closed at infinity by one singular, perspective added point at projective infinity. As example, $U(1)$ is projected down to the octonion 7 tangent on its south pole from ∞ sitting at its north pole, 2-dimensional S^2 is similarly projected down to the tangent xy -plane by rotation. From P_3 the R^3 cell coordinates are used. Interpreted is st as a central projection, having a parameter t and constant a as length on a vertical z -axis. If the central projection with coordinates (0,0, a) maps a space point (x,y,z) with coordinate $z < a$ down to the xy -plane, the image has projective coordinates $[-ax, 0, z-a]$. This applies also to st_1 (or st_2) which maps S^1 down to $[x, 0, 1-z]$.

The projective norming is $[1, 0, (z-1)/x]$. Using substitutions and scaling, the last coordinate is $(z-1)/z$ or $(r-R_s)/r$, the Moebius transformation for rotations or the Schwarzschild factor. The coefficient matrix G is of order 6 for the G -compass and color charge force on the octonian e_0 coordinate. It has as units setting eigenvector $(-p_2, 1)$, p_2 a complex third root of unity. A translation transformation can be for $[x, 1, z] \rightarrow [x, 0, 1-z]$ with first row $(-1 \ 0 \ 0)$, second row $(0 \ 0 \ 0)$ and third row $(0 \ -1 \ 1)$.

Consider now the option R_4 for $(x,y,\phi_0,6b)$. Fiber bundles are other projections. $SU(2): S^3$ as unit sphere in R^4 has the Hopf projection onto S^2 as fiber bundle map with fiber S^1 . Extended $SU(3): S^5$ has S^1 as fiber for its fiber bundle with base CP^2 . If a higher dimensional twisted bundle is invented, S^9 in a complex C^5 space maps down to S^5 as topological factor of the $SU(3)$ geometry. Its fiber is S^3 replacing S^1 . The toroidal $S^3 \times S^5$ geometry of $SU(3)$ replaces the torus in S^3 for leptons charge location. A latitude circle in S^2 has its points blown up by S^1 to a 45-degree leaning, rotating circle on the torus surface $S^1 \times S^1$. Fiber bundle maps are added to projective correlations, changing dimensions.

The phase changing angle $\phi_0 \ 2g$ from above was used in [1] by the parity operator P for setting an angle β as rescaling factor $\cos^2\beta$ for the Minkowski to the Schwarzschild metric. This gives orthogonal, spiralic projections mentioned for 1234 as Hilbert space H , also for Minkowski rescaling with $\sin \phi = v/c$, v relativistic speed (Figure 6). With the two cusp parameters as $z_5 = (\phi_0, 6b) = z_1 \times z_2 \times z_3 \times z_4$ the real space R^5 is extended to the complex space C^5 . $z_4 = z_1 \times z_2 \times z_3$ is for the octonions 07, z_3 was for mass, frequency (m,f) 56. For real H as R^4 the metric is Euclidean $\langle u, u \rangle$, for C^4 Hermitian. The Minkowski rescaling for spacetime is due to a Morse function M having critical points: to the Euclidean $\langle u, u \rangle$ metric is applied the time reversal operator T , for instance in reduced $u = (r, ct)$ coordinates to $\langle u, u \rangle = r^2 - c^2 t^2$ as equation $r^2 = c^2 t^2$ for the Minkowski light cone. Catastrophes with thresholds (here for the T application), sudden changes, jumps apply also to CPT. As catastrophe thresholds for the setting of T (also C) can be used the fold for T with maximum level for a $+$ sign and counterclockwise rotations mp_0 , $-$ sign for clockwise cw rotations, also for the change between left- and right-handed space orientations, using base vector determinants. In the Lorentz transformations T changes the sign of the speed between two coordinates as $+v$ or $-v$. From the CPT operators of physics, the operator C is for complex conjugation and changing all quantum numbers of a quanta system as sudden changes. The CPT symmetry is $Z_2 \times Z_2$ with $C = PT = TP$. P applications are coordinate point rotations $u \rightarrow \lambda u$, $|\lambda| = 1$, for real, complex or quaternionic u -coordinates. P has associated the cusp catastrophe. The thresholds are also for their sudden changes (Figure 4). Multiplication with λ for P is a coordinate base vector rotation (or point- reflection), a matrix operator using λ . For C as complex z conjugation $c(z)$ the Pauli matrix σ_1 generates with the Hopf map application the vector $u = (z^2 = x + iy, 1)$ to $u\sigma_1(1, c(z^2))$ $tr = z^2 c(z^2) = x^2 + y^2 = r^2$ for the complex distance measure. It is also obtained by the reflection $(x, iy) \rightarrow (x, -iy)$.

Matrix operations as transformations (used for the C operator as σ_2 matrix example) are used, replacing catastrophes. The standard models symmetry $U(1) \times SU(2) \times SU(3)$ is not catastrophe bound [7]. The symmetries set in addition eigenvectors of their matrices as force vectors

for energies. For the three forces they come as 1,3,8 symmetry generators of $U(1)$, $SU(2)$, $SU(3)$. GR has the Moebius transformations MT as symmetry of the Riemannian sphere S^2 . The invariants are six cross ratios as matrices for the six color charges. Potential functions f_s s-parametrized sets are replaced by $\exp(i\varphi)$ having one variable and one field quantum photon, three WI Pauli matrices for three weak bosons, transmitting energies or acting for decays, 8 SI gluons in a quark-gluon plasma, confining with the gluon exchange between quarks them in nucleons. For EM magnetic field quanta replace the former field quantum's for electrical charge and potential in 14, 145. For rotations as energy the cc force on e_0 can act as symmetry in 03, 037. For 126 as field quantum for GR with mass 5 acts 4-dimensional 1256 as local GR field projection into 1234 about a mass system. $U(1)$ has 7, 167 associated;

kinetic energy and momentum $p = mv$ have 6, 356 the SI rotor associated [5]; heat as energy 2 and GF 246 has density of matter in a volume V associates generating pressure on the volumes (spherical) surface. In the last case, the state change of matter between solid, fluid and gas remind again to catastrophes with a triple point and three cusps in superposition, using 126. They appear for instance in the butterfly geometry for 1246 as parameters and one variable 4 added. Two cusps superposition appear in the swallowtail (1 variable, 3 parameters) geometry, an application is for research; it can be for $[x, y, \varphi_0, \lambda]$. The case of 4 cusp superpositions appears in figure 3 related to GR. The elliptic umbilic is associated with the 6-roll mill and the SI rotor, for the WI wheel also. The parabolic umbilic (2 variables and 4 parameters) was associated with GR, the swallowtail is contained in it.

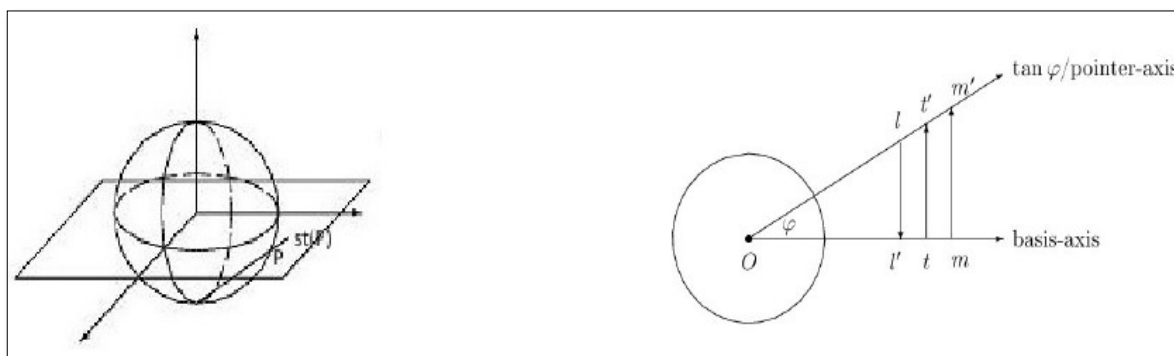


Figure 6. Stereographic (or central) projection, orthogonal (cosine) projection as Minkowski rescaling of energy measures.

Dihedral decays

In the above geometrical considerations, the shapes of decayed systems P are not discussed. In the 9Tool bag are 12 demonstration models and videos for inner dynamics are also available. As a Heegaard decomposition Tool for S^3 are here added dihedrals. The WI S^3 can decay into two systems like an electron and an antineutrino, coming from the decay of a W^- boson. The genus 0 case lets a weak boson decay into two solid, 3-dimensional balls with a bounding sphere S^2 . These can be two copies for two atoms location in spacetime. Hopf spheres for electrons are several copies of S^2 , discrete available as shells using main quantum numbers. From genus 1 on, the reduced coordinate presentation is by a circle with $n = 1, 2, 3, \dots$ points in the distance of n th roots of unity marked. They act for 0-dimensional poles carrying an energy or charge. In the 3-dimensional decay blow up for a system P , P has n toroidal handles with a disk E_j removed. A central sphere has n discrete disks removed and at each such boundary is attached an E_j for the P shaped bounding manifold and its homotopy or homology generators. Their higher dimensional generators are not discussed here. In retracts, they are 1-dimensional (**Figure 7**, Lissajous figures). Beside presentations of equipotential and field lines (**Figure 2**), the inner dynamics of flows in P is guided by

the number of poles, demonstrated as rotating rolls which are driven (for even n) mostly in pairs by a common force as motor. The dihedral D_0 is $U(1)$, S^1 with no characteristic polynomial for n th roots. The dihedral D_1 has genus 1 for a torus and the characteristic polynomial $z - 1$; the conjugation operator for its symmetry of order 2 is for oriented rotations. D_2 for POT (electrical, mass/GR potentials) is for quark brezel genus 2 lemniscates with characteristic polynomial $z^2 - 1$. The inner dynamics of all D_n with characteristic polynomial $z_n - 1$ uses finite, cyclic Fibonacci-like difference equation solutions. They replace differential equations. For quarks the 2-roll mill of catastrophe theory applies, the 4-roll mill D_4 is for a weak bosonic inner flow rotation, the 6-roll mill D_6 as G-compass (figure 3) is for color charges and inner nucleon flows. The nucleons three quarks handle body of genus 3 as D_3 is for the SI rotor presentation. The n th roots use often for their finite Fibonacci sequence solutions the powers of eigenvector numbers, belonging to characteristic polynomials. As numbers occur -1 in $(-1)^n$ with values $\{+1, -1\}$, as p_1 or p_2 , third roots of unity with values $\{1, p_1, p_2\}$ or signed as $\{+1, -1, +p_1, -p_1, +p_2, -p_2\}$ for the 6 roll mill, for $n = 4$ as $\{1, i, -1, -i\}$ for the 4 roll mill, also assigned 8th roots of unity. The mills are described in

catastrophe theory by potential functions, having 1 or 2 variables and 1-4 parameters.

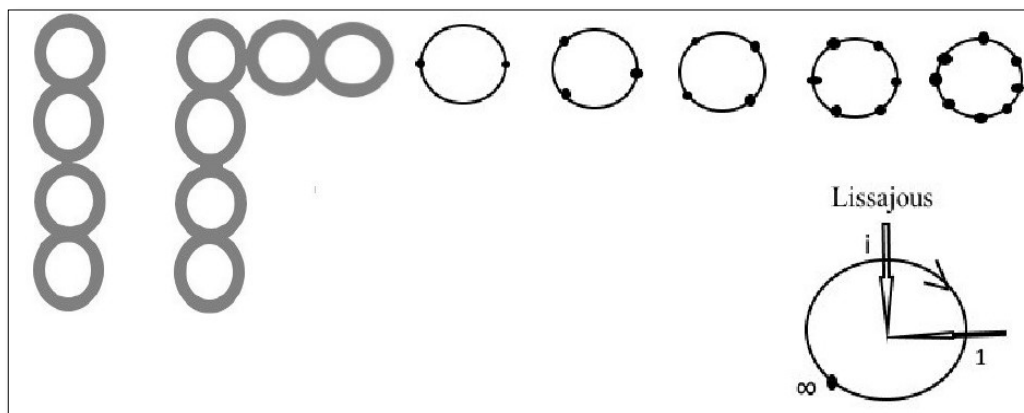


Figure 7. Heegaard decompositions genus 4, 6 toroidal handles, dihedral for poles, Lissajous figure.

CONCLUSION

Concerning decays: The Higgs decay makes in the first step the 5-dimensional Higgs field [8]. It can set quarks as energy quantum's having the two potentials EM (pot), E(pot) unified in the Higgs field. Quarks decay by generating weak bosons and they decay (for instance) in two leptons or two photons. Atomic kernel AK decays arise through the forming of proton-neutron Cooper pairs in AK having an isospin exchange. When the pairs get at too large distance in AK, nuclear decay occurs [9,10]. Concerning sudden changes in systems: catastrophes appear can give thresholds for state changes in systems and state changes are also due to applying symmetry transformation matrices [11-19]. Geometry oriented settings are discussed with models for demonstrations. Dihedrals are one tool for shapes of decay systems. A Tool bag exists which demonstrates many facts for the quanta range.

REFERENCES

- Kalmbach GHE (2017) Einstein metrics and two projection maps. MINT-WIGRIS. MINT Verlag, Bad Woerishofen.
- Kalmbach GHE (2020) (Chef-Hrsg) MINT (Mathematik, Informatik, Naturwissenschaften, Technik). MINT Verlag; Bad Woerishofen. pp: 1-65.
- Poston T, Stewart I (1978) Catastrophe theory and its applications. Pitman; London.
- Internet video under YouTube: Moebius Transformations Revealed; 2014.
- Kalmbach GHE, Eberspaecher U (2019) MINT-Wigris Tool Bag; Bad Woerishofen.
- Kalmbach GHE (2020) MINT-Wigris Postulates. In: researchgate.net 2020 under MINT-Wigris Project
- Stierstadt K (1989) Physik der Materie. VCH; Weinheim.
- Schmutzer E (2004) Projektive einheitliche Feldtheorie. Harry Deutsch; Frankfurt.
- MINT-Wigris project (G. Kalmbach H.E.), in the internet under: researchgate.net.
- Kalmbach GHE (2020) A Heisenberg c-compass. J Appl Mater Sci Eng Res 4(2): 63-67.
- Thompson JMT, Hunt GW (1979) A bifurcation theory for the instabilities of optimization and design. In: Berlinski D. (ed.), Mathematical Methods in the Social Sciences.
- Thompson JMT, Gaspar ZA (1977) A buckling model for the set of umbilic catastrophes. (preprint, Eng. Dept. Univ. College, London).
- Thompson JMT, Hunt GW (1973) General Theory of Elastic Stability. Wiley; NewYork.
- Bell GM, Lavis DA (1978) Thermodynamic phase changes and catastrophe theory.
- Stanley HE (1971) Introduction to Phase transitions and critical phenomena. Oxford Univ. Press; London.
- Wald A (1957) On some systems of equations of mathematical economics. Econometrica 19: 368-408.
- Howard IN (1975) Bifurcations in reaction-diffusion problems. Adv Math 16: 246-258.
- Berry MV (1976) Waves and Thom's theorem. Adv Physics 25: 1-25.